

Differentiation of CD3⁻4⁻8⁻ Human Fetal Thymocytes In Vivo: Characterization of a CD3⁻4⁺8⁻ Intermediate

By Daniel L. Kraft,* Irving L. Weissman,[§]|| and Edmund K. Waller*[‡]

From the *Cancer Biology Research Laboratory, and the Departments of [‡]Medicine, [§]Pathology, and ^{||}Developmental Biology, Stanford University School of Medicine, Stanford, California 94305

Summary

Human thymocyte differentiation was examined by injecting fetal thymic progenitor populations into human thymic xenografts in SCID-hu mice. Thymic progenitors were fluorescently labeled with the lipophilic dye PKH2. The phenotypes of their progeny could be identified by flow cytometric analysis of cells with a very high fluorescent PKH2 signal. Intrathymic injection of purified triple negative (TN) CD3⁻4⁻8⁻ thymocytes resulted in the sequential appearance of CD3⁻4⁺8⁻, CD3⁻4⁺8⁺, and CD3⁺4⁺8⁺ cells, with the subsequent appearance of small numbers of phenotypically mature CD3⁺4⁺8⁻ and CD3⁺4⁻8⁺ cells over a 4-d period. Sorted CD3⁻4⁺8⁻ thymocytes injected intrathymically rapidly differentiated to CD4⁺8⁺ cells. CD4⁺8⁺ fetal thymocytes in cell cycle differentiated into phenotypically mature CD3⁺4⁺8⁻ and CD3⁺4⁻8⁺ populations, whereas nondividing CD4⁺8⁺ cells failed to differentiate after intrathymic transfer. The number of cell divisions that occurred between the injection of TN thymocytes and their progeny at different time points was estimated based on the decrease in the intensity of the PKH2 label. The average length of the cell cycle for the TN population was calculated to be 24 h. The SCID-hu model thus provides a useful tool for studying the kinetics of cell division and differentiation of human thymocytes in vivo.

A major site of T lymphocyte differentiation is the thymus (for a review see reference 1). CD3⁻4⁻8⁻, triple negative (TN)¹ (or in some cases CD3⁻4^{lo}8⁻ [2]) thymic progenitors from the bone marrow (3), fetal liver, and yolk sac have been shown in mice (4, 5) and humans (6, 7) to migrate to the thymus where they undergo maturation and differentiation. In vivo studies of murine thymocytes have demonstrated differentiation of TN thymocytes to mature CD3⁺4⁺8⁻ and CD3⁺4⁻8⁺ single positive populations via immature CD3⁻4⁻8⁺ followed by CD4⁺8⁺ intermediates (8, 9). The fate of most developing thymocytes is intrathymic death, either early through a failure of the TCR expressed on the cell surface to be engaged by its self-MHC, or later in maturation through a process by which self-reactive thymocytes are eliminated, termed negative selection (10–13). Before or concomitant to negative selection, CD4⁺8⁺3^{lo} cells that are specific for self-MHC undergo positive selection to develop

into T cells that express high levels of TCR in association with the CD4 or CD8 coreceptor, and which are capable of interacting with antigen bound to self-MHC (10, 14–16). Thymocytes that have successfully passed through positive and negative selection develop into TCR^{hi} T cells with mature phenotypes, emigrate to the periphery, and home to peripheral lymphoid organs (17–19). The kinetics of cell division and differentiation during these processes have been partially defined in murine systems (20–23), and to our knowledge, have not been described for human T cell development.

Previous descriptions of human thymocyte subpopulations presumably involved in differentiation in vivo have largely been restricted to flow cytometric analysis of antigen expression on human fetal and postnatal thymuses obtained at different points during embryogenesis and postnatal development (24) or immunohistochemical analysis of fetal and postnatal thymocytes (25), both static models that do not define progenitor–progeny relationships in a lineage. Attempts to study the differentiation of human TN thymocytes in vitro have yielded contradictory results, with some reports showing evidence of partial differentiation of fetal thymocytes, (26–29) whereas in other studies, postnatal thymocytes failed to

¹ Abbreviations used in this paper: APC, allophycocyanin; DP, double positive; NCS, normal calf serum; PI, propidium iodide; SA, Streptavidin; TR, Texas red.

differentiate in vitro (30). The discrepancies among these studies may be due to the limitations inherent in in vitro model systems, as thymic stromal microenvironments have been shown to play a crucial role in mediating the differentiation of thymocytes (31–36).

Until recently, models for an in vivo stromal microenvironment in which to study human hematopoiesis and thymocyte differentiation were lacking. The SCID-hu mouse provides such a model for the in vivo study of components of the human immune system (37). Human fetal thymic xenografts, transplanted under the SCID mouse kidney capsule with fragments of fetal liver, develop into thymic organs that have a similar histology to that of human postnatal thymus (37, 38), and provide a system where dynamic events of T cell differentiation can be measured (39).

We herein report studies on the in vivo differentiation of purified human T cell progenitor populations that were injected intrathymically into allogeneic human thymic xenografts in SCID-hu mice. To identify injected donor thymic progenitors, injected cells were labeled with PKH2, a stable, fluorescent dye that incorporates into the cell membrane. The intensity of PKH2 fluorescence was shown to be dependent upon the number of cell divisions that followed labeling. Analysis of the relative fluorescence of PKH2⁺, donor-derived cells in the SCID-hu thymus and their pattern of CD3, CD4, and CD8 expression elucidated the frequency of cell division and at least one pathway of differentiation from CD3⁻4⁻8⁻ thymocytes to those with more mature phenotypes. The results show that in this model, human fetal TN thymocytes have the capacity for self-renewal, as well as differentiation via a CD3⁻4⁻8⁻ intermediate, to CD3⁻4⁺8⁻/CD3⁺4⁺8⁺ populations and mature CD3⁺4⁺8⁻ and CD3⁺4⁻8⁺ subsets.

Materials and Methods

Mice. SCID-hu mice were prepared as previously described (38) by engrafting small fragments of human fetal thymus and liver grafts under the left kidney capsule of 4–6-wk-old C-B17 *scid/scid* mice. Fetal liver served as a source of hematopoietic progenitor cells. SCID-hu mice were maintained under filter tops in the Stanford University research animal care facility. Tissues were obtained from aborted fetuses of 17–22 wk gestational age after consent of the patients and approval of the Institutional Review Board of Stanford University Medical Center on the use of Human Subjects in Medical Research. Engrafted mice were used 2–4 mo after engraftment, a time at which the human thymic tissue had grown to more than 100 times the original volume (40).

mAbs and Fluorescent Reagents. Murine antibodies to human CD3, CD4, CD5, CD7, CD8, CD10, CD15, CD19, CD20, CD25, CD30, CD34, CD38, CD43, CD45, Leu-8, and HLA-DR were obtained from Becton Dickinson & Co. (San Jose, CA). Streptavidin-conjugated Texas red (SA-TR) and allophycocyanin (APC) were purchased from Caltag Laboratories (San Francisco, CA). APC-anti-CD5 was a generous gift of Drs. Neelima Bhat and Aaron Kantor (Stanford University Medical School, Stanford, CA). FITC anti-CD34 and APC-conjugated anti-CD8 were gifts of Dr. Leon Terstappen (Becton Dickinson & Co., San Jose, CA).

Isolation of Fetal Thymocyte Subpopulations. TN thymocytes were enriched by negative selection before flow cytometric cell sorting by magnetic bead depletion of mature thymocytes as described in

detail elsewhere (8, 41, 42). Briefly, thymocytes suspended at 2×10^8 /ml in 5 mmol/liter HBSS, pH 7.4 containing 5% vol/vol heat-inactivated normal calf serum (NCS), and 0.02% wt/vol sodium azide (Gibco Laboratories, Grand Island, NY) were depleted of marker positive cells by incubation with biotinylated mAbs to CD3, CD4, and CD8, followed by the addition of paramagnetic beads coated with SA ($100 \mu\text{l}/10^8$ cells; Advanced Magnetics, Inc., Cambridge, MA) for 30–60 min at 4°C with constant mixing. Bead-coated thymic cells were then removed by magnetic separation, and the remaining cells restained with biotinylated antibodies to CD3, CD4, and CD8, followed by SA-TR. To enrich for CD3⁻4⁺8⁻ cells, magnetic bead depletion with biotinylated anti-CD3 and anti-CD8 mAb was followed by staining with SA-TR and PE anti-CD4. CD3⁻4⁻8⁻ and CD3⁻4⁺8⁻ cells were sorted separately by setting the appropriate electronic gates for CD3⁻8⁻ cells and sorting either PE-negative (CD3⁻4⁻8⁻ cells) or PE-positive populations (CD3⁻4⁺8⁻ cells). FITC-conjugated anti-CD45 or APC-conjugated anti-CD5 mAbs were included in the final staining step in order to identify the T cell progenitors (which are CD45^{lo} and CD5^{lo}) in the CD3⁻4⁻8⁻ TN population. Most of the thymic B cells and all of the thymic macrophages in the fetal thymus were excluded from sorts of T cell progenitors, by virtue of their lack of expression of the CD5 marker (in the case of conventional CD5⁻ B cells and macrophages) or their higher level of CD45 expression than CD3⁻4⁻8⁻ T cell progenitors (in the case of all thymic B cells and macrophages). In some experiments in which APC-conjugated anti-CD5 mAb was used to identify the T cell progenitors, a low level of contamination of the TN population with CD5⁺ thymic B cells could not be excluded. However, separate FACS[®] analyses (Becton Dickinson & Co.) including a variety of T and B cell markers, demonstrated that CD5^{lo} CD19⁺ thymic B cells comprise <11% of the CD5^{lo} CD3⁻4⁻8⁻ TN population. TN and CD3⁻4⁺8⁻ cells were sorted by setting appropriate electronic gates with the highly modified dual-laser FACS[®] system (Becton Dickinson & Co.) equipped with a four-decade logarithmic amplifier (43). When PKH2 cell labeling preceded cell sorting, electronic gates in the FITC channel were set in such a way that a homogeneously labeled, highly fluorescent population was obtained (see below). After sorting, an aliquot of the sorted cells was reanalyzed, and in all experiments described, the degree of purity was $\geq 98\%$.

PKH2 Labeling of Thymocytes. Just before or after cell sorting, TN-enriched, bead-depleted thymocytes or sorted TN and CD3⁻4⁺8⁻ cells, respectively, were labeled with 4 μM PKH2 (Zynaxis Cell Science Inc., Malvern, PA), a stable, fluorescent dye that incorporates into the cell membrane. PKH2 has an excitation peak of 490 nm and an emission peak of 504 nm. The FITC fluorescence channel was used to measure PKH2 levels. Thymocytes labeled with 4 μM PKH2 have a fluorescence in the FITC channel more than 10 times that of cells labeled with saturating concentrations of directly conjugated FITC mAb such as FITC-anti-CD4. Thymocytes in conical, polypropylene tubes were washed once at room temperature in HBSS or PBS containing no serum or sodium azide. Cells were then resuspended in Zynaxis buffer A ($1\text{--}2 \times 10^6$ thymocytes/ml) and an equal volume of 8 μM PKH2 (diluted in buffer A) was added to the cells. Cells were incubated in the resultant 4 μM PKH2 with frequent mixing for 2 min. Staining was terminated by adding an equal volume of NCS, followed by dilution of labeled cells with HBSS. PKH2-labeled cells were then washed three times by dilution with HBSS, underlaying with NCS, and centrifugation for 10 min at 4°C, 200 g, before FACS[®] sorting or injection into SCID-hu thymic xenografts.

Intrathymic Injections. SCID-hu mice were anesthetized with a

mixture of xylazine (17 $\mu\text{g/g}$ body weight; Mobay Corporation, Shawnee, KA) and Ketaset (ketamine HCl, 83 $\mu\text{g/g}$ body weight; Parke-Davis, Morris Plains, NJ). The SCID-hu thymus graft that had been previously placed beneath the capsule of the left kidney was exposed via a lateral incision and injected with 10^5 – 10^6 sorted, PKH2-labeled thymocytes in 10–30 μl of HBSS using a gas-tight syringe (Hamilton Co., Reno, NV) and a 30-gauge needle. Sham-injected control grafts were injected with HBSS alone. The wound was then closed with a 4-0 nylon suture and surgical staples.

Flow Cytometric Analysis of Human Thymocytes from SCID-hu Mice. Cell surface staining and flow cytometric analysis of lymphoid cells was performed with cell suspensions of SCID-hu thymus xenografts that had been injected previously with sorted, PKH2-labeled progenitor populations. Cells were labeled with saturating concentrations of biotinylated anti-CD3 plus SA-TR, PE-conjugated anti-CD4, and APC-conjugated anti-CD8, or unlabeled anti-CD3 followed by goat anti-mouse Ig TR, PE anti-CD4, and biotinylated anti-CD8 plus SA-APC. At each staining step, antibodies were mixed with cells at 4°C for 20 min in HBSS containing 5% NCS in 50–200 μl vol. Multicolor immunofluorescent analysis of cell suspensions in HBSS/NCS (plus 1 $\mu\text{g/ml}$ propidium iodide (PI), or without PI for fixed cells and those combinations of labeled antibodies using both the PE and APC channels) were performed by FACS[®]. In three-color analysis, dead cells were excluded from the analysis by normal scatter gating methods and by setting electronic gates to exclude PI-positive cells (43). In four-color analysis, dead cells were excluded only by forward and obtuse scatter gating. Computer-generated contour plots from fluorescent measurements of viable cells were used to present the two-color staining patterns. The number of contour lines drawn in a particular area represents the frequency of cells exhibiting a given level of fluorescence, where the area contained between any two lines represents 5% of the total cell population. The contour plots are labeled according to the established names of the molecules detected by the particular antibodies (e.g., CD4, CD8).

Detection of Donor-derived Thymocytes. Because of the small proportion of donor-derived cells in SCID-hu grafts, PKH2-positive cells made up <0.5% of cell suspensions from intrathymically injected SCID-hu grafts. Analysis of donor-derived PKH2-positive cells was achieved by collecting data on cells with a mean PKH2 fluorescent signal of more than 25 (channel 140), which was 40 times greater than that of the mean fluorescent signal of unlabeled thymocytes (0.6; channel $30 \pm \text{SD } 20$ channels), using a four-decade scale divided into 250 channels such that a difference of 70 channels represents a 10-fold difference in fluorescent signal intensity, and a difference of 20 channels represents a twofold difference in the mean fluorescent signal intensity. Less than .002% (1/50,000) of lymphoid cells in sham-injected control thymus grafts had fluorescent signals greater than the threshold of 25 (channel 140). For analysis of PKH2-labeled cells, cells with PKH2 fluorescence of greater than 25 were counted as being derived from the injected, PKH2-labeled thymocytes. Cells from injected thymic grafts were analyzed for CD3, CD4, CD8, and the signal intensity of the PKH2 label. PI and forward and obtuse scatter gates were used to exclude dead and nonlymphoid cells.

Hoechst Staining and Sorting for Dividing CD4⁺8⁺ Thymocytes. To differentiate and sort between nondividing and dividing CD4⁺8⁺ thymocytes, fetal thymocytes were labeled with the vital DNA stain, HOECHST-33342 (bisBenzimide H-33342; Sigma Chemical Co., St. Louis, MO) (44). Thymocytes were first labeled with FITC-conjugated anti-CD4 and PE-CD8. Cells were concentrated by centrifugation, then resuspended in HBSS without sodium azide, and warmed to 37°C for 15 min. HOECHST 33342

dye and PI were then added at final concentrations of 5 and 1 $\mu\text{g/ml}$, respectively. After a 30-min incubation at 37°C, cells were sorted for CD4⁺8⁺ HOECHST-negative (cells in G₀₋₁) and -positive (cells in S/G2+M, with greater than 2N DNA content) by setting and appropriate electronic gates. Sorting was performed with a FAC-Star II[®] flow cytometer (Becton Dickinson & Co.) equipped with two argon lasers, one emitting at 488 nm for detection of FITC, PE, and PI, and the other in the UV region for detection of HOECHST 33342. Dead cells were excluded by gating on forward and obtuse scatter and PI.

Results

PKH2 Signal Intensity Can Be Used to Measure the Rate of Cell Division. The relationship between the decline of fluorescence signal from PKH2-labeled cell populations and cell division was established in vitro by labeling a human B cell lymphoma cell line (LM919) (Waller, E. K., unpublished observations) with PKH2 and measuring the number of labeled cells and their PKH2 signal intensity at various times thereafter. Each doubling of the number of labeled cells corresponded to a 50% drop in the mean fluorescent signal as the dye present in the plasma membrane of the parent cell was divided among two daughter cells (Fig. 1). Others have observed the same relationship with PKH2 labeling and division kinetics (45), and have also demonstrated that (a) the PKH2 dye results in uniform staining of the plasma membrane; (b) the dye does not leak out of cells; (c) it is not transferred from cell to cell within the same culture; and (d) the growth rate and metabolic activity of PKH2-labeled cells are unaffected compared with unstained controls (46).

PKH2-labeled Human Thymocytes Injected into SCID-hu Thymic Xenografts Were Identified as a Distinct, Highly Fluorescent Population upon Analysis by Flow Cytometry. Intrathymically injected thymocytes (enriched for immature TN thymocytes to a purity of 50% by CD3, CD4, and CD8 magnetic bead depletion and labeled with PKH2) could be easily identified in the FITC channel as a separate, highly fluores-

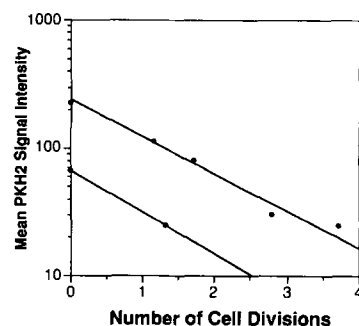


Figure 1. PKH2 signal correlates with cell division. A human B cell lymphoma cell line (LM919) was labeled with either 4 μM (upper curve) or 2 μM (lower curve) PKH2 and plated in separate wells of a 24-well dish at a concentration of $5 \times 10^6/\text{ml}$. At 24 h, the cells in one well were counted, and their mean PKH2 signal intensity was determined by flow cytometry. The number of cell divisions was determined by calculating for γ (cells/ml = original No. of cells/ml $\times e^\gamma$) where γ divided by 0.693 = number of divisions. The fractional decrease in PKH2 signal intensity per cell division was calculated from an exponential curve fit.

cent population at various time points after injection (Fig. 2). In this experiment, the fraction of PKH2-labeled cells varied between 1 and 10% of the total thymocytes in the injected grafts. The signal intensity of fluorescently labeled cells (represented as the mean fluorescent signal of the population of PKH2⁺ cells) declined exponentially with time, suggesting that cell division was occurring within the PKH2-labeled population.

Developmental Potential of CD3⁻4⁻8⁻ Thymocytes In Vivo. To determine the developmental fate of thymocytes at defined stages of differentiation, different thymic populations were sorted to a purity of >98%, PKH2 labeled, and injected into SCID-hu thymic grafts. The TN cells, present in the fetal thymus at a frequency of 1–4% (Fig. 3 A), were sorted (Fig. 3 B) and analyzed for their expression of CD34. At least 50% of sorted TN cells were CD34⁺ (Fig. 3 C). TN cells were labeled with PKH2 (Fig. 3 D) and injected into the thymic grafts of SCID-hu mice. The pattern of CD3, CD4, and CD8 expression on the PKH2-labeled population of fetal thymocytes was determined at 12, 24, 48, 72, and 96 h after their injection into thymic grafts. Data from a control graft analyzed without a gate on PKH2⁺ cells (Fig. 3 E), a graft analyzed 24 h after injection (with an electronic gate to display the phenotype of PKH2⁺ cells) (Fig. 3 F) and a graft analyzed 48 h after injection (Fig. 3 G) are shown from a representative experiment. The pattern of differentiation from several experiments was identical: the rapid appearance of a CD3⁻4⁺8⁻ population followed by CD3⁻4⁺8⁺ and CD3⁺4⁺8⁺ populations, and the appearance of small numbers of phenotypically mature CD3⁺4⁺8⁺ and CD3⁺4⁻8⁻ cells. The data from six separate experiments were similar and are summarized in Fig. 4. The fraction of

PKH2-labeled thymocytes recovered that remained TN (Fig. 4 A) decreased from 100% at the time of injection, to a mean of 90% at 12 h, 55% at 24 h, 29% at 72 h, and 7% at 96 h. The initial appearance, after 12–24 h, of a CD3⁻4⁺8⁻ population (Fig. 4 B) suggest that TN thymocytes differentiate in vivo via a CD3⁻4⁺8⁻ intermediate population. The increase in the fraction of PKH2-labeled thymocytes recovered that were CD3⁻4⁺8⁻, was followed by an increase in the fraction of PKH2⁺ cells that were CD4⁺8⁺ (Fig. 4 C). Small numbers of PKH2-labeled, donor-derived thymocytes with mature phenotypes (CD3⁺4⁺8⁻ and 3⁺4⁻8⁺) were apparent by 48 h (Fig. 4 D). Their percentage of the total population of donor-derived PKH2-labeled cells approached the relative frequency of these cells in the normal thymus.

CD3⁻4⁺8⁻ Thymocytes Differentiate to CD4⁺8⁺ Thymocytes In Vivo. If the CD3⁻4⁺8⁻ population is a true sequential intermediate between TN and CD4⁺8⁺ double positive (DP) thymocytes in human T cell differentiation, it should be present in normal human fetal thymus. Flow cytometric analysis of both fetal and SCID-hu thymocytes revealed the presence of a significant CD3⁻4⁺8⁻ population (2–4% of thymocytes) (Fig. 5 A, CD4⁺8⁻, upper left panel, and Sen-Majumdar, A., Stanford University Medical Center, Stanford, CA, unpublished observations). Significant numbers of CD3⁻4⁻8⁺ cells were not detected in analysis of human fetal thymus (Fig. 5 A, CD4⁻8⁺, lower right panel). Further characterization of human fetal CD3⁻4⁺8⁻ thymocytes revealed these cells to be CD1⁺, CD2⁺, CD5^{int-hi}, CD7⁺, CD38⁺, CD43⁺, CD45⁺, CD10⁻, CD15⁻, CD20⁻, and CD25⁻, and predominantly HLA-DR⁻ and L-selectin (Leu-8)⁻. As CD4 expression increases in the CD3⁻8⁻ population, there was a concomitant de-

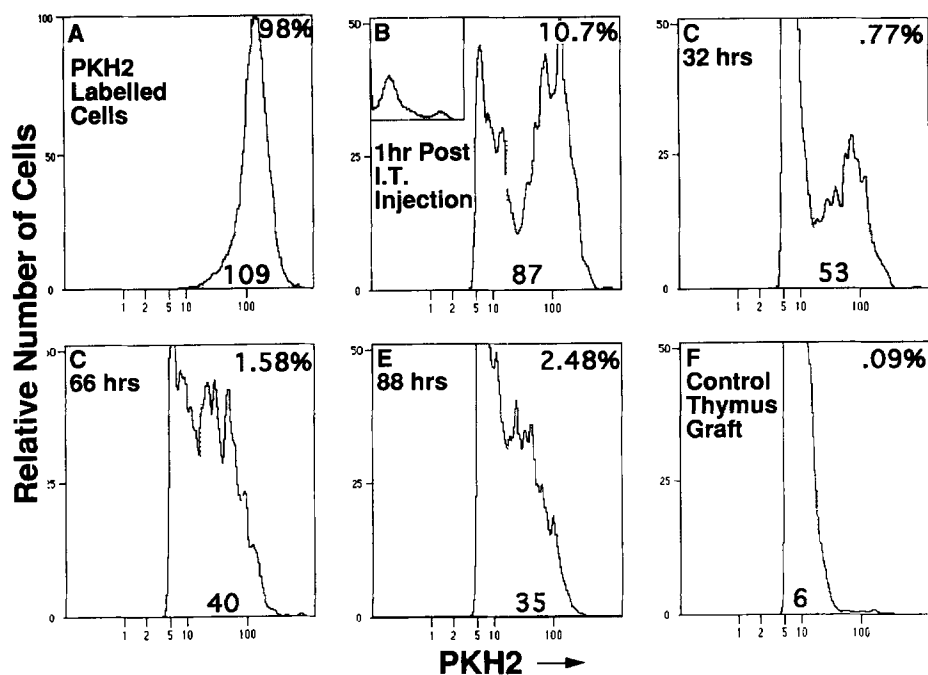


Figure 2. (A) 5×10^6 PKH2-labeled fetal thymocytes enriched for TN (to a purity of 50% by bead depletion) were injected into separate SCID-hu thymic grafts. At various time points after injection, thymocytes from injected and control grafts were analyzed for their PKH2 signal intensity (B–E). To simplify data analysis, only data on cells with a PKH2 signal greater than 6 (channel 100) were collected (B, inset). Thymocytes from sham-injected control thymuses never had a significant PKH2 signal greater than 25 (channel 140) (F). The percentage of thymocytes from each graft with a PKH2 signal greater than 25 (channel 140) is shown in each panel (top right). (Bottom) Absolute mean fluorescent signal intensities (on a scale of 0.1–1,000).

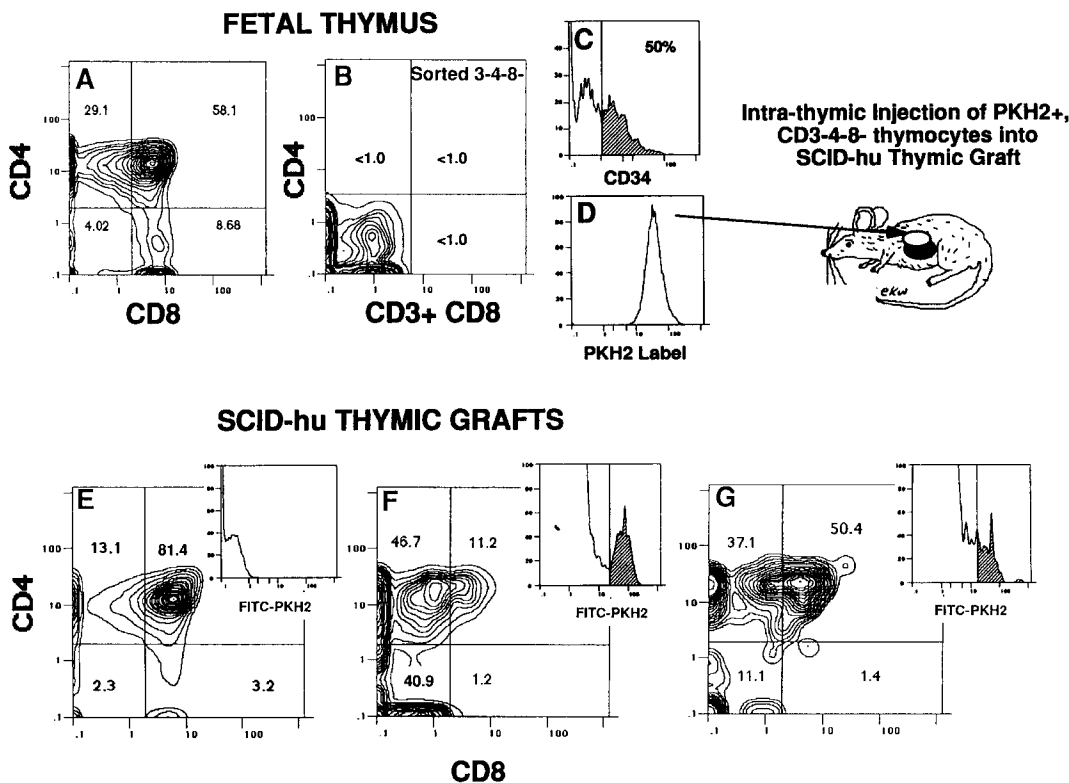


Figure 3. CD3⁻4⁻8⁻ thymocyte differentiation in vivo. A representative experiment in which a 20-wk fetal thymus (A) was sorted for TN thymocytes, as described in Materials and Methods. The TN cells were sorted and reanalyzed by FACS[®] (B). 50% of the TN cells expressed high levels of CD34 (C). These sorted TN cells were uniformly labeled with PKH2 (D) and were injected intrathymically into the thymic xenografts of SCID-hu mice. The CD4 vs CD8 profile of all thymocytes in the recipient graft (E), and the profiles of PKH2⁺, donor-derived thymocytes from grafts analyzed at 24 (F) and 48 (G) h are shown. The density profile of PKH2 signal of injected grafts is shown (F and G, inset) and the fraction of thymocytes that were PKH2⁺ (and therefore, donor derived) is shaded. The relative percentages of recovered PKH2⁺ thymocytes of different phenotypes are shown in each quadrant. At 24 h the ratio of CD3⁻ to CD3⁺ in the PKH2⁺ CD4⁺8⁻ population was 88:12; the corresponding ratio for the CD4⁺8⁺ population was 77:23. At 48 h the ratios of CD3⁻ to CD3⁺ cells had decreased to 70:30 (CD4⁺8⁻) and 71:18 (CD4⁺8⁺).

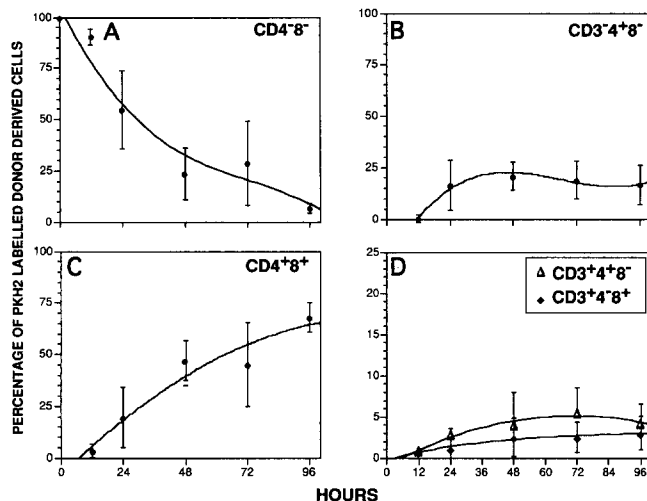


Figure 4. In vivo differentiation after transfer of PKH2-labeled CD3⁻4⁻8⁻ TN fetal thymocytes to SCID-hu thymic xenografts. The TN subpopulation of fetal thymocytes was sorted and labeled with PKH2 as described in Materials and Methods. At 12, 24, 48, 72, and 96 h after intrathymic transfer, thymocytes from the recipient thymus were analyzed for expression of CD3, CD4, CD8, and PKH2 label by four-color flow

cytometry. Data were gated for PKH2 positive, donor-derived cells (PKH2 signal intensity >25; channel 140). Percentages represent the mean fraction of PKH2 positive, donor-derived thymocytes expressing different T cell phenotypes that were recovered at various time points after TN injection. Error bars represent SD.

cytometry. Data were gated for PKH2 positive, donor-derived cells (PKH2 signal intensity >25; channel 140). Percentages represent the mean fraction of PKH2 positive, donor-derived thymocytes expressing different T cell phenotypes that were recovered at various time points after TN injection. Error bars represent SD.

increase in expression of CD34, a marker of human hematopoietic precursor cells (24, 47), such that CD3⁻4^{hi}8⁻ thymocytes were predominantly CD34⁻ (Fig. 5 B). Fetal CD3⁻4⁺8⁻ thymocytes were sorted, labeled with PKH2, and injected intrathymically into SCID-hu xenografts. The majority of PKH2-labeled 3⁻4⁺8⁻ cells underwent rapid differentiation into both CD3⁻4⁺8⁺ and CD3⁺4⁺8⁺ cells (Fig. 6), with over 67% of the recovered PKH2-labeled thymocytes expressing both the CD4 and CD8 markers 48 h after intrathymic injection. Small numbers of donor-derived, phenotypically mature CD3⁻4⁺8⁻ and CD3⁺4⁻8⁺ cells were evident after 24–48 h in vivo.

The Subpopulation of CD4⁺8⁺ Thymocytes in Cell Cycle Differentiate to Mature CD3⁺4⁺8⁻ and CD3⁺4⁻8⁺ Cells whereas Nondividing CD4⁺8⁺ Cells Fail to Differentiate. Previous work from this laboratory (10) demonstrated in mu-

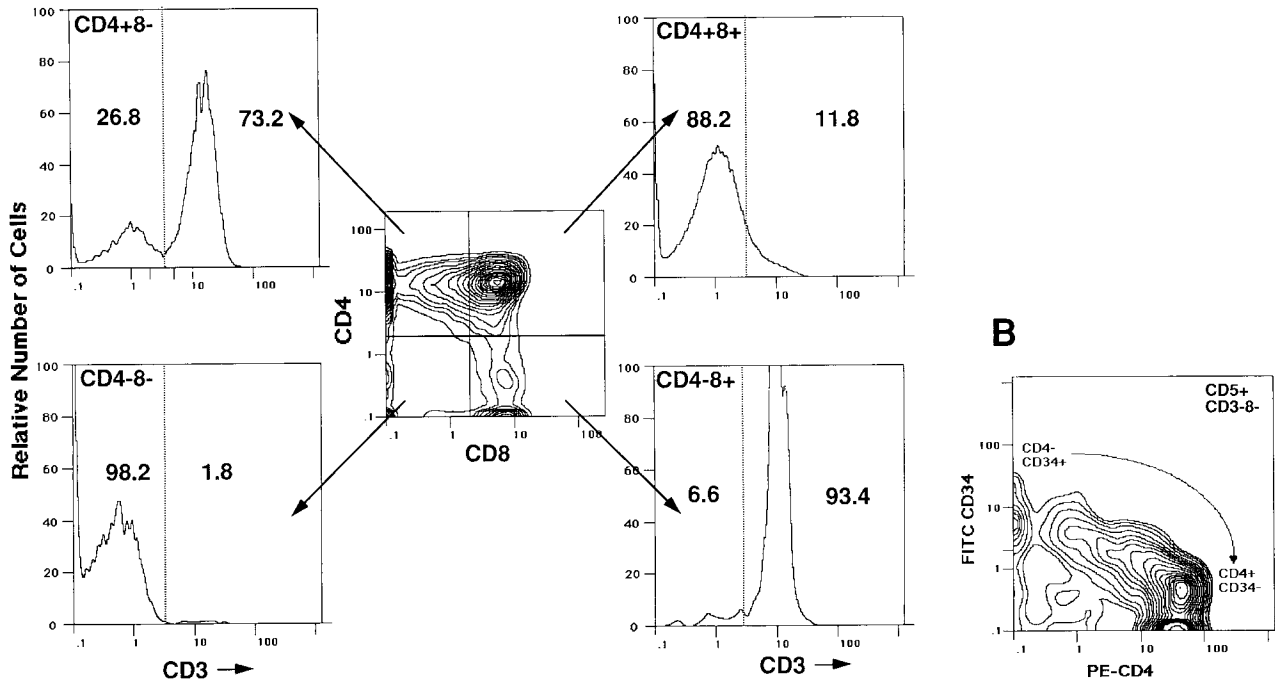


Figure 5. CD3⁻4⁺8⁻ cells constitute a small population in the normal human fetal thymus. (A) The CD3 profiles of CD4⁻8⁻, CD4⁺8⁻, CD4⁺8⁺, and CD4⁻8⁺ thymocytes are shown, with the percentages of CD3⁻ and CD3⁺ cells shown. (B) The CD34 and CD4 profile of the CD5⁺3⁻8⁻ population of fetal thymocytes.

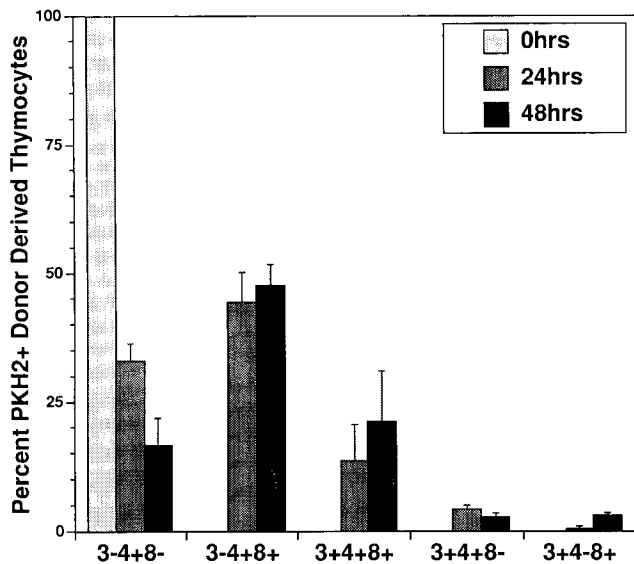


Figure 6. CD3⁻4⁺8⁻ thymocytes differentiate intrathymically into CD4⁺8⁺ thymocytes. Sorted, PKH2-labeled CD3⁻4⁺8⁻ fetal thymocytes were injected into SCID-hu thymic grafts. Donor-derived thymocytes were analyzed by flow cytometry 24 and 48 h after injection. The fraction of recovered PKH2-labeled, donor-derived thymocytes in each thymocyte subpopulation at each time point is shown. Values are derived from the means of three separate experiments.

rine thymocyte development that CD4⁺8⁺ blast cells possessed the capacity to differentiate into mature cells, whereas small, nonblastic DP thymocytes remained DP or died in vivo. We isolated dividing CD4⁺8⁺ human fetal thymocytes by sorting those DP thymocytes with greater than 2 N DNA content (in S/G2+M) as measured by HOECHST 33342 staining (Fig. 7 A). Cells containing >2 N DNA content had a scatter profile consistent with that of dividing cells, and were larger than cells with 2 N DNA content (data not shown). Sorted, HOECHST 2 N PKH2-labeled 4⁺8⁺ cells were observed to remain predominantly DP thymocytes when analyzed up to 48 h after IT injection into SCID-hu thymus grafts (Fig. 7 B). Less than 5% of the donor-derived cells recovered after transfer had differentiated to mature single positive phenotypes. Sorted CD4⁺8⁺ that were in cell cycle (HOECHST-positive cells with >2 N DNA content) showed evidence of differentiation into both CD3⁺4⁺8⁺ (13.7% of the recovered PKH2⁺ cells) and 3⁺4⁺8⁻ (12.3% of the recovered PKH2⁺ cells) phenotypically mature single positive populations (Fig. 7 C).

Cell Division Kinetics of CD3⁻4⁺8⁻ Thymocytes. The decline in fluorescent signal intensity of PKH2-labeled cells corresponded with the number of cell divisions those cells had undergone (Fig. 1), and therefore it is reasonable to assume that the decline in PKH2 label intensity with time could be

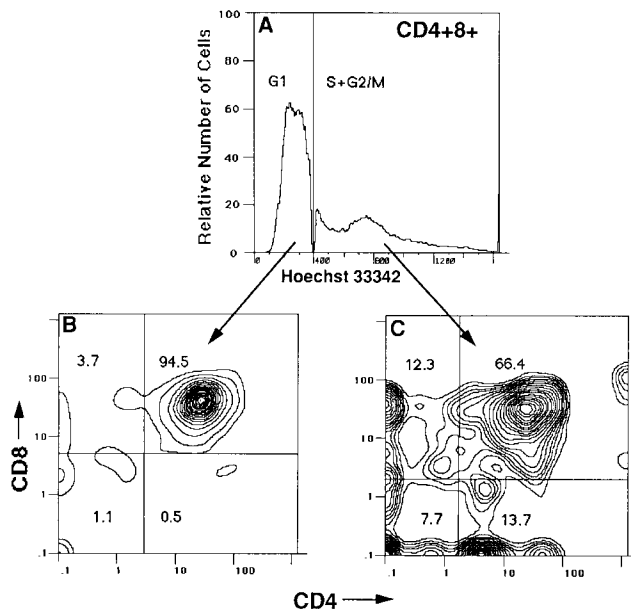


Figure 7. CD4⁺8⁺ thymocytes in cell cycle differentiate to mature CD3⁺4⁺8⁻ and CD3⁺4⁻8⁺ cells whereas nondividing CD4⁺8⁺ cells fail to differentiate after transfer to SCID-hu thymus grafts. (A) CD4⁺8⁺ HOECHST 33342 labeled thymocytes were sorted on the basis of DNA content. After sorting and labeling with PKH2, HOECHST 2 N (G₀-G₁) and HOECHST >2 N (S/G₂+M) CD4⁺8⁺ thymocytes were injected into SCID-hu thymic grafts. 48 h later, injected grafts were analyzed and the CD4 vs. CD8 profile of PKH2⁺ cells derived from donor DP 2 N (B) and DP HOECHST >2 N cells (C) is shown. Numbers in each quadrant show the percentages of respective donor-derived populations.

used to estimate the rate of cell division for defined human thymocyte populations. The mean fluorescent signal of the donor-derived PKH2-labeled TN cells declined exponentially with respect to time after intrathymic injection, and the decline in the natural logarithm of the mean fluorescent signal of the PKH2-labeled cells that remained TN was nearly linear in each experiment (Fig. 8 A). However, the data points in Fig. 8 A did not fit perfectly on a straight line. In particular, the initial slope of the line connecting the first two data points in each experiment was steeper than the line that was the best curve fit for all the data points. These data were best approximated by a series of second degree polynomial equations, in which $y = c \cdot x^2 - (m \cdot x) + b$, where y is the \ln [PKH2 signal] at time x , b is the \ln [PKH2 signal] at time 0, and c and m are constants related to the rate of cell division in the TN population, and the fraction of cells in cell cycle, and x is time, in days. We calculated that the initial decline in the \ln [PKH2 signal] during the first 24 h from a mean of five experiments to be $-0.7 \pm 0.17 \ln$ [PKH2 signal]/day, which corresponds to a 50% decrease in the PKH2 signal/day, and a calculated cell cycle length for the TN population of 24 ± 6 h (the PKH2 signal decreases 50% during each cell division; Fig. 1). This calculation assumes that the PKH2-labeled TN population is homogeneous with respect to the rate of cell division and the fraction of cells in cell cycle during the first 24-h period after injection.

To compare the number of cell divisions that thymocytes of various phenotypes (CD3⁻4⁻8⁻, CD3⁻4⁺8⁻, CD3⁻4⁺8⁺, CD3⁺4⁺8⁺) had experienced during their dif-

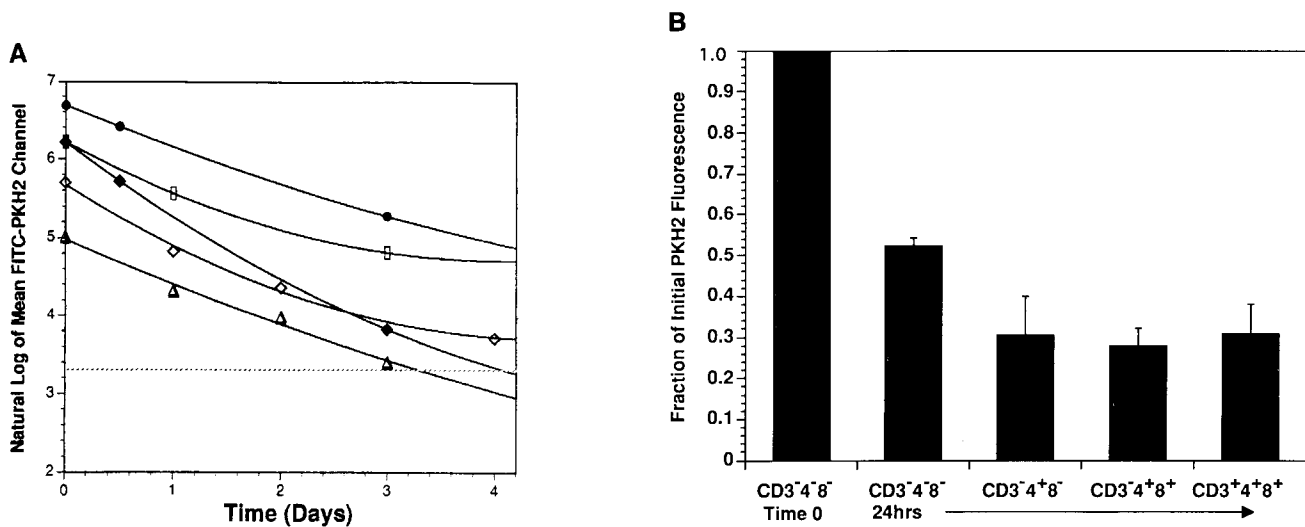


Figure 8. The mean PKH2 signal intensity in TN donor-derived populations decreased over time. (A) The natural logarithm of the PKH2 fluorescence signals from five separate experiments in which several SCID-hu grafts were injected with the same population of PKH2-labeled TN thymocytes and analyzed at different time points are plotted. The initial intensity of PKH2 labeling in the TN population varied by experiment. The data points were best modeled by second degree polynomial equations in which the decline in the \ln [PKH2 signal] initially is nearly linear during the first 24 h, and is then followed by a progressively lower rate of decline over the next 3 d. The initial slopes of the decline in the \ln [PKH2 signal] for the TN population were calculated for each experiment at 24 h, with a mean value of $-0.7 \pm 0.17 \ln$ [PKH2 signal]/day, which is equivalent to a 50% decrease in the PKH2 signal/day, and yields an estimated cell cycle length for the TN population of 24 ± 6 h (the PKH2 signal decreases 50% during each cell division; Fig. 1). (Dashed line) Highest level of background fluorescent signal measured in control thymic grafts. (B) The mean PKH2 signal intensity of donor-derived thymocyte population at 24 h as a fraction of the initial PKH2 signal intensity of the TN thymocytes that were injected into the SCID-hu thymus graft.

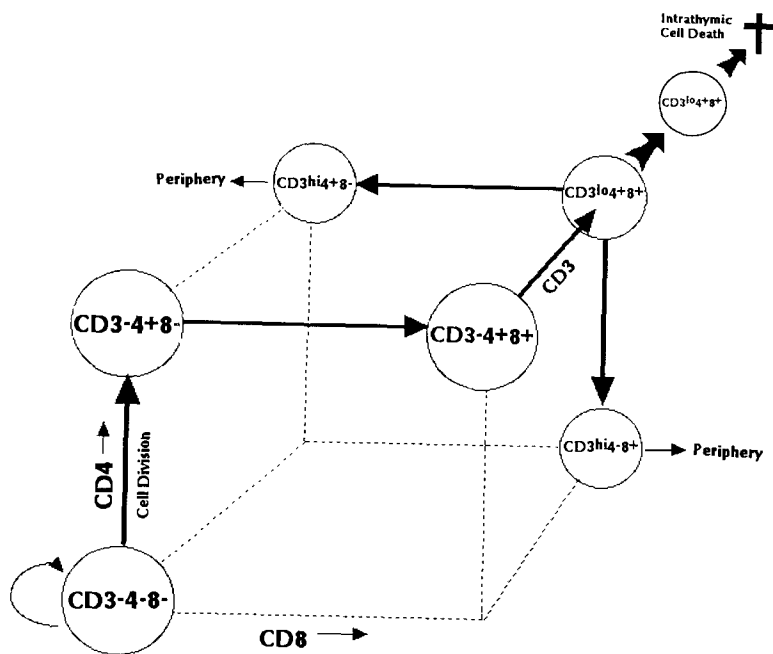


Figure 9. A model for the differentiation of $CD3^{-}4^{-}8^{-}$ human fetal thymocytes. Some TN thymocytes show evidence for self-renewal. Other TN thymocytes differentiate to a rapidly dividing $CD3^{-}4^{+}8^{-}$ population, which results in subsequent appearance of $CD3^{-}4^{+}8^{+}$ and $CD3^{+}4^{+}8^{+}$ populations. Most of the $CD3^{+}4^{+}8^{+}$ population undergoes intrathymic death whereas a fraction differentiate into mature $CD3^{+}4^{+}8^{-}$ and $CD3^{+}4^{-}8^{+}$ thymocytes.

ferentiation from PKH2-labeled TN cells, their mean fluorescent (PKH2) signals were calculated as fractions of the initial fluorescent signal of the PKH2-labeled TN thymocytes that had been previously injected. Whereas the fluorescent signal of the TN cells declined at a nearly constant exponential rate in each experiment, presumably as a result of their cell division (Fig. 8 A), some of their thymic progeny showed a greater rate of decrease in their PKH2 signals. As shown for donor-derived thymocytes analyzed 24 h after intrathymic injection, the PKH2 signal in the TN population declined to 50% of that of the input cells, whereas the PKH2 signal of the more mature thymocyte subpopulations ($CD3^{-}4^{+}8^{-}$, $CD3^{-}4^{+}8^{+}$, $CD3^{+}4^{+}8^{+}$) had declined to $\sim 30\%$ of the input value (Fig. 8 B), suggesting that, on the average, these cells had undergone approximately one more cell division than the corresponding TN cells.

Discussion

This study provides direct information regarding the phenotypes and differentiation pathway of human thymic progenitors *in vivo*. In this report, we have transferred T cell progenitors at defined stages of development into SCID-hu thymic grafts and described their intrathymic differentiation into phenotypically more mature populations. We used the fluorescent dye, PKH2, to mark donor cells and their progeny *in vivo* and to distinguish them from the unlabeled thymocytes present in the SCID-hu thymic grafts. Congenic markers are not available for human thymocytes, such as Thy 1.1 and 1.2 used in murine studies (8, 9), nor was it feasible to identify thymic T cell progenitors through the use of host/donor HLA mismatch, (used to distinguish mature progeny of $CD34^{+}$, hematopoietic stem cells in long-term reconstitution assays

in SCID-hu mice [48]) because of the low expression of HLA by immature thymocytes.

The system of marking thymic progenitors and their progeny with PKH2 has the advantage of being easy to perform and results in the fluorescent marking of donor-derived cells in a way that allows an approximation of the number of cell divisions they have undergone. However, we noted three technical limitations with this method. First, only a finite number of cell divisions can be followed in labeled progeny before the level of PKH2 signal intensity becomes indistinguishable from that of background fluorescence (Fig. 8 A), and the variance in the PKH2 signal intensity in the donor-derived thymocytes increased with time. Cells with an initial mean PKH2 fluorescence of 320, for example, could undergo four cell divisions before dilution of the PKH2 in derivative cells would fall below the highest level of background autofluorescence seen in host thymocytes. The variance in the mean PKH2 signal of different thymic subsets can be attributed to the variance in the original PKH2 staining intensity of the labeled TN population and a variable number of cell divisions that occurred between the PKH2-labeled TN and their progeny.

A second technical drawback to this system, though not directly related to PKH2 staining, was that the recovery of PKH2-labeled TN cells and their progeny was low. Since each thymus graft contained different numbers of total thymocytes, and the actual number of PKH2⁺ cells injected successfully into the graft varied among different grafts within a given experiment, the absolute numbers of PKH2⁺ cells and their fraction of the total thymocyte population [number injected/(number injected + number host thymocytes)] varied considerably. After injection of a mean (\pm SD) of $248,000 \pm 117,000$ PKH2-labeled TN into thymic grafts that con-

tained a mean of $36 \times 10^6 \pm 21 \times 10^6$ cells, the absolute number of PKH2-labeled cells that could be detected at different time points in thymic grafts varied from a mean of $27,340 \pm 3,400$ cells at 12 h (a recovery of 16% of the number of PKH2⁺ cells injected) to $19,280 \pm 9,500$ at 24 h (11.2% recovery); $11,799 \pm 6,200$ at 48 h (10.2% recovery); $25,860 \pm 17,100$ at 72 h (7.4% recovery); and $21,800 \pm 9,200$ at 96 h (6.7% recovery). These data indicate that only about 10–20% of the pKH2-labeled TN cells that we attempted to inject into the graft remained as viable cells at 12 h, and their PKH2-labeled progeny constituted a slowly declining fraction of the total thymocytes in the graft thereafter. The large initial loss of PKH2-labeled cells immediately after intrathymic injection suggests that a majority of the injected cells fail to remain in the thymus (they leak out of the injection site), or that they die soon after injection, an observation that is true for direct in situ intrathymic injection studies (49).

The failure to observe an accumulation of PKH2-labeled cells 12–96 h after intrathymic injection may be due to the emigration of mature thymocytes into the peripheral circulation of the SCID-hu mouse (17, 18, 37); their intrathymic cell death, either at the level of CD3^{lo}CD4⁺CD8⁺ cells (due to the failure of antigen-presenting cells to engage the TCR [16]), or at the level of CD3⁺CD4⁺CD8⁻ or CD3⁺CD4⁻CD8⁺ (due to negative selection) (10); or a competition between the self-renewal of PKH2-labeled TN and the endogenous production of TN thymocytes within the SCID-hu thymic graft. SCID-hu thymic grafts contain an admixture of thymocytes and pluripotent hematopoietic stem cells (7) derived from fragments of fetal liver, and thus have a relatively constant supply of new TN thymic progenitors. Therefore we would predict that the proportion of PKH2-labeled thymocytes would diminish over time as PKH2⁺-labeled TN cells mature, differentiate, and/or die, and are replaced by unlabeled TN cells derived from fetal liver hematopoietic stem cells.

The third technical point concerning this system was that we studied the differentiation of fetal thymocytes in heterologous (HLA mismatched) thymus grafts in SCID mice. We used fetal thymus as a source of thymic progenitors because they contained greater numbers of immature thymocytes than were present in established SCID-hu grafts. The differentiation of hematopoietic stem cells to mature T cells after their injection into heterologous thymic grafts has been demonstrated (50), indicating the ability of thymocyte progenitors, mismatched with respect to their expression of HLA antigens compared with the recipient thymus (51), to differentiate normally in SCID-hu mice (6, 48). In these experiments, the mature, donor-derived thymocytes had normal phenotypes and were tolerant to the HLA presented by the thymic-host stromal environment (52). Nevertheless, the differentiation of T cell progenitors in an allogeneic, HLA mismatched thymic microenvironment might differ from the differentiation of T cell progenitors in an autologous thymic microenvironment. Therefore, we sorted TN thymocytes from SCID-hu grafts, labeled them with PKH2, and injected the PKH2-labeled TN cells into SCID-hu mice that had been grafted

with thymic tissue from the same fetal donor. We found immature TN thymocytes made up a smaller proportion (<0.2%) of thymocytes in SCID-hu grafts 2 mo after engraftment as compared with 1–3% TN cells of human fetal thymus. The differentiation of the limited number of TN cells that could be sorted from SCID-hu grafts occurred in an identical pattern as that we have observed with fetal thymocytes (data not shown).

CD34 has been shown to be a marker of human hematopoietic stem cells (6, 24, 47, 48) as well as the earliest thymic T cell progenitor (24). We characterized the phenotype of the TN and CD3⁻CD4⁺CD8⁻ progenitors from fetal thymus with respect to their expression of CD34 and other lymphoid markers. We found that TN thymocytes expressed intermediate levels of the CD5, CD45, and HLA-DR antigens (CD5^{lo}CD45^{lo}HLA-DR^{lo}). Greater than 50% of the sorted TN cells were CD34⁺ and lacked significant expression of HLA class I antigens. In contrast, more mature T cell phenotypes were CD34⁻CD5^{hi}, and CD45^{hi}. CD34 expression was inversely correlated with CD4 expression (Fig. 5 B). Low levels of CD4 expression have recently been described on a population of murine pluripotent hematopoietic stem cells (53). CD34⁺ cells present in the CD3⁻CD4⁺CD8⁻ population (which fell between TN and CD3⁻CD4⁺CD8⁻ cells, the latter being CD34⁻) could warrant consideration in future studies of human thymocyte differentiation.

We observed the maturation of CD3⁻CD4⁺CD8⁻ progenitors to more mature thymocytes in vivo, with the sequential appearance of CD3⁻CD4⁺CD8⁻, CD3⁻CD4⁺CD8⁺, CD3⁺CD4⁺CD8⁺, CD3⁺CD4⁺CD8⁻, and CD3⁺CD4⁻CD8⁺ populations over 12–96 h. Differentiation of murine TN to mature thymocyte subsets in vitro, on short-term thymic stromal cultures, has also recently been shown to occur within 2 d (54, 55). Using the system of PKH2-labeling thymocyte progenitors, we have observed differentiation of the most immature (TN) thymocyte to cells with the most mature (single positive) phenotype. At 24, 48, and 72 h after injection of PKH2-labeled TN, there were approximately twice as many PKH2-labeled CD3⁺CD4⁺CD8⁻ cells compared with CD3⁺CD4⁻CD8⁺ thymocytes, although the total fraction of phenotypically mature thymocytes never rose above 10% of the entire PKH2-labeled population (Fig. 4 D). The relative ratio of PKH2-labeled CD4 and CD8 single positive thymocytes at the latter time points were similar to those seen in SCID-hu thymic grafts in which the ratio of phenotypically mature CD3⁺CD4⁺CD8⁻ and CD3⁺CD4⁻CD8⁺ cells was slightly more than 2:1, with CD4⁺ single positives comprising $12 \pm 7\%$ of thymocytes, and CD8 single positive thymocytes comprising $5 \pm 6\%$ of the thymocyte population (17).

The exponential decline in PKH2 signal of donor-derived TN thymocytes suggested that TN cells retained the potential for limited self-renewal, since a proportion of the TN progeny cells remain phenotypically TN, and demonstrate progressively lower intensities of the PKH2 label, consistent with cell division (Figs. 1 and 8 A). Based on the initial rate of decline of the ln[PKH2 fluorescence signal] of donor-derived PKH2-labeled TN thymocytes at 24 h after intrathymic injection, we estimated the length of the cell cycle for the TN

population to be 24 ± 6 h (Fig. 8 A). This calculation assumes that the PKH2-labeled TN cells constitute a uniform population with respect to the fraction of cells in cell cycle and their cell cycle length. After the *in vivo* growth of PKH2-labeled TN cells, the variance of their fluorescent signal is too large to detect subpopulations of PKH2-labeled TN cells that could have different cell cycle kinetics. Thus the average cell cycle length of 24 h, that we calculated for the TN population as a whole, could represent a combination of shorter and longer cell cycle lengths of subpopulations of TN that are dividing more and less rapidly, respectively. The change in the slope of the decline in the \ln [PKH2 signal] at later time points (Fig. 8 B) suggests that the PKH2-labeled TN population is indeed somewhat heterogeneous, and contains a subpopulation(s) of cells that are nondividing, or dividing at a slower rate. Therefore, the decline of the \ln [PKH2 signal] is best approximated by a second degree polynomial equation rather than a first degree polynomial (linear) equation. As the PKH2-labeled TN differentiated, they constituted a diminished fraction of the total PKH2⁺ population. We have estimated that, on the average, $\sim 30\%$ of the TN cells differentiate into more mature cells, whereas 70% of the progeny remain phenotypically TN after each cell division.

Compared with the corresponding TN population, the lower intensities of PKH2 label in the thymocyte populations of intermediate differentiation ($CD3^{-4+8^{-}}$, $3^{-4+8^{+}}$, and $3^{+4+8^{+}}$) 24 h after intrathymic injection of PKH2-labeled TN thymocytes, suggested that either (a) more cell divisions had occurred in these thymic subpopulations compared with those TN cells that remained phenotypically unchanged; or (b) the subpopulations of TN that differentiate to more mature phenotypes undergo more rapid cell division than those PKH2-labeled cells that remain phenotypically TN (Fig. 8 B). Conclusions from several studies on murine thymocyte kinetics (20–23) which demonstrate more rapid cell cycling in the $CD3^{-4-8^{+}}$ population compared with the more immature TN population (23) support the idea that thymocytes of intermediate levels of differentiation (between TN and the phenotypically mature cells) may divide more rapidly than the TN population (56).

After the injection of PKH2-labeled TN cells, a PKH2-labeled $CD3^{-4+8^{-}}$ population rapidly appeared in the thymus, largely preceding the appearance of larger numbers of $CD3^{-4+8^{+}}$ and $CD3^{+4+8^{+}}$ cells (Figs. 3 F, 4 B and 4 C). Sorted, PKH2-labeled $CD3^{-4+8^{-}}$ cells differentiated rapidly *in vivo*, to $CD3^{-4+8^{+}}$ and $CD3^{+4+8^{+}}$ populations (Fig. 6), indicating that the $CD3^{-4+8^{-}}$ population was a sequential intermediate between TN and $CD3^{-4+8^{+}}$ / $CD3^{+4+8^{+}}$ populations. These results are in contrast to the differentiation of mouse thymocytes in C57BL strains, in which the differentiation of TN thymocytes proceeds primarily through a $CD3^{-4-8^{+}}$ intermediate to the $CD4^{+8^{+}}$ population (9), but are similar to the pathway described in CBA mouse strains, in which TN differentiate through a $3^{-4+8^{-}}$ intermediate as well (57–59). Murine $CD3^{-4-8^{+}}$ and $CD3^{-4+8^{-}}$ thymocytes have been shown to be large, blast cells, cortisone sensitive, and concentrated in the outer cortex (60).

Spitz et al. (26) have demonstrated that the human postnatal $3^{-4+8^{+}}$ population can be subdivided into $CD3^{-4+8\alpha^{-}8\beta^{-}}$ and $CD3^{-4+8\alpha^{+}8\beta^{+}}$ populations, and that the expression of $CD8\alpha^{+}$ precedes the expression of $CD8\beta$ when TN thymocytes are cultured *in vitro*. These authors noted a $CD3^{-4+8\alpha^{-}}$ population, that is presumably identical to the $CD3^{-4+8^{-}}$ population described in the present study, as we have used an antibody to CD8, Leu-2a, that recognizes $CD8\alpha$. An additional pathway of human thymic differentiation from $CD3^{-4-8^{-}}$ cells to $CD4^{+8^{+}}$ without going through the $CD3^{-4+8^{-}}$ immature intermediate is possible, and cannot be excluded by our data. However, at least 50% of TN thymocytes appear to mature via a $CD3^{-4+8^{-}}$ intermediate (Fig. 4). In addition, small numbers of $CD3^{+4-8^{-}}$ cells appeared at later time points, which contributed to the overall $CD4^{-8^{-}}$ population. Because of the rarity of the $CD3^{+4-8^{-}}$ cells, the developmental pathway that leads to this thymic subset could not be determined.

The maturation of human TN thymocytes *in vivo* via a $CD3^{-4+8^{-}}$ intermediate correlates well with *in vitro* differentiation studies of TN and $CD3^{-4+8^{-}}$ thymocytes on short-term, heterologous, human-stromal cell cultures (Lieberman, M., A. Sen-Majumdar, D. L. Kraft, I. L. Weissman, and E. K. Waller, unpublished observations).

The expression of CD4 at an early stage of intrathymic T cell maturation could potentially play a role in HIV infection of the thymus (61). This is testable, as SCID-hu thymic grafts sustain productive HIV infection (62), and in the infected thymuses, eventual depletion of $CD4^{+}$ cells occurs (62a). Furthermore, a rapidly cycling immature $CD3^{-4+8^{-}}$ intermediate may play a role in lymphomagenesis. An inducible murine T cell lymphoma corresponding to the immature murine $CD3^{-4-8^{+}}$ thymocyte subset has recently been reported (63). Two $CD3^{-4+8^{-}}$ human lymphomas have recently been described in immunosuppressed organ transplant recipients, and may represent the neoplastic analog of the $CD3^{-4+8^{-}}$ thymic intermediate (64).

The technique of FACS[®] sorting based on relative DNA content (HOECHST staining) combined with PKH2 labeling, allowed an investigation of the relative potential of dividing vs. nondividing populations to differentiate. $CD4^{+8^{+}}$ cells were sorted on the basis of their DNA content, PKH2 labeled, and injected into thymic grafts (Fig. 7). The subpopulation in cell cycle (DNA content $>2N$) differentiated into thymocytes of a mature phenotype, whereas $CD4^{+8^{+}}$ cells not engaged in DNA synthesis failed to differentiate to a significant degree *in vivo* (Fig. 6). It has been reported that the majority of dividing mouse $CD4^{+8^{+}}$ blasts express low levels of TCR/CD3 (65). Taken together, these data indicate that the nondividing subset of small $CD4^{+8^{+}}$ cells are destined to die intrathymically, and that only those $CD4^{+8^{+}}$ cells that have received mitogenic stimuli (presumably as a result of engagement of the low numbers of TCR expressed on their surfaces) are able to differentiate further into thymocytes of more mature phenotypes (positive selection) (10).

Fig. 9 presents a model for a differentiation pathway of human TN fetal thymocytes which summarizes our data. The ability to observe human T cell differentiation *in vivo* pro-

vides a means to examine the developmental ontogeny of TN thymocyte populations of more defined phenotypes (such as CD34⁺ pediatric and adult thymocytes). Other developmental phenomena can be examined, such as extrathymic T cell differentiation, and the effects of systemic/physiologic variables on thymocyte differentiation (39).

Intrathymic transfer of PKH2-labeled human thymocyte

populations into the SCID-hu mouse model offers a useful *in vivo* model for the study of short-term human T cell differentiation. Use of such a system should prove useful in the delineation and ontogeny of various progenitor cell populations in the thymus, and other human tissues that can be engrafted into SCID mice (66).

The authors wish to acknowledge Drs. Anish Sen-Majumdar and Miriam Lieberman for their support and critical reading of the manuscript; Dr. Sen-Majumdar for sharing his unpublished observations on the phenotype of the CD3⁻4⁺8⁻ thymic population; and Dr. Susan Alpert for useful discussions. Special thanks go to Gun Hansteen, Tim Knaak, the FACS[®] facility personnel, and Ryan Seay for technical help.

D. L. Kraft was supported by a Howard Hughes Medical Institute Research training fellowship for medical students. I. L. Weissman was supported by National Institutes of Health grant CA-42551. E. K. Waller is a McDonnell Scholar, and this work was supported by the James S. McDonnell Foundation.

Address correspondence to Dr. E. K. Waller, Becton Dickinson Immunocytometry Systems, 2350 Qume Drive, San Jose, CA 95131-1807.

Received for publication 31 December 1992 and in revised form 5 April 1993.

References

- Adkins, B., C. Mueller, C.Y. Okada, R.A. Reichert, I.L. Weissman, and G.J. Spangrude. 1987. Early events in T-cell maturation. *Annu. Rev. Immunol.* 5:325.
- Wu, L., R. Scollar, M. Egerton, M. Pearse, G.J. Spangrude, and K. Shortman. 1991. CD4 expressed on earliest T-lineage precursor cells in the adult murine thymus. *Nature (Lond.)* 349:71.
- Spangrude, G.J., C.E. Muller-Sieburg, S. Heimfeld, and I.L. Weissman. 1988. Two rare populations of mouse Thy-1^b bone marrow cells repopulate the thymus. *J. Exp. Med.* 167:1671.
- Weissman, I., V. Papaioannou, and R. Gardner. 1978. Fetal hematopoietic origins of the adult hematomorphoid system. Cold Spring Harbor Meeting on Differentiation of Normal and Neoplastic Hematopoietic Cells. B. Clarkson, P.A. Marsk, and J.E. Till, editors. 33-47.
- Owen, J.J., and E.J. Jenkinson. 1984. Early events in T lymphocyte genesis in the fetal thymus. *Am. J. Anat.* 170:301.
- Baum, C.M., I.L. Weissman, A.S. Tsukamoto, A. Buckle, and B. Peault. 1992. Isolation of a candidate human hematopoietic stem-cell population. *Proc. Natl. Acad. Sci. USA.* 89:2804.
- Peault, B., I.L. Weissman, C. Baum, J.M. McCune, and A. Tsukamoto. 1991. Lymphoid reconstitution of the human fetal thymus in SCID mice with CD34⁺ precursor cells. *J. Exp. Med.* 174.
- Guidos, C.J., I.L. Weissman, and B. Adkins. 1989. Developmental potential of CD4⁻8⁻ thymocytes. Peripheral progeny include mature CD4⁻8⁻ T cells bearing $\alpha\beta$ T cell receptor. *J. Immunol.* 142:3773.
- Guidos, C.J., I.L. Weissman, and B. Adkins. 1989. Intrathymic maturation of murine T lymphocytes from CD8⁺ precursors. *Proc. Natl. Acad. Sci. USA.* 86:7542.
- Guidos, C.J., J.S. Danska, C.G. Fathman, and I.L. Weissman. 1990. T cell receptor-mediated negative selection of autoreactive T lymphocyte precursors occurs after commitment to the CD4 or CD8 lineages. *J. Exp. Med.* 172:835.
- Kappler, J.W., N. Roehm, and P. Marrack. 1987. T cell tolerance by clonal elimination in the thymus. *Cell.* 49:273.
- Fowlkes, B.J., R.H. Schwartz, D.M. Pardoll, W. Swat, M. Dessing, A. Baron, P. Kisielow, and H. von Boehmer. 1992. Phenotypic changes accompanying positive selection of CD4⁺8⁺ thymocytes. *Eur. J. Immunol.* 22:2367.
- Fowlkes, B.J., R.H. Schwartz, and D.M. Pardoll. 1988. Deletion of self-reactive thymocytes occurs at a CD4⁺8⁺ precursor stage. *Nature (Lond.)* 334:620.
- von Boehmer, H. 1992. Thymic selection: a matter of life and death. *Immunol. Today.* 13:454.
- Borgulya, P., H. Kishi, U. Muller, J. Kirberg, and H. von Boehmer. 1991. Development of the CD4 and CD8 lineage of T cells: instruction versus selection. *EMBO (Eur. Mol. Biol. Organ.) J.* 10:913.
- Robey, E.A., B.J. Fowlkes, J.W. Gordon, D. Kiousis, H. von Boehmer, R. Ramsdell, and R. Axel. 1991. Thymic selection in CD8 transgenic mice supports an instructive model for commitment to a CD4 or CD8 lineage. *Cell.* 64:99.
- Weissman, I.L. Thymus cell migration. 1967. *J. Exp. Med.* 126:291.
- Scollay, R., M. Kochen, E. Butcher, and I.L. Weissman. 1978. Lyt markers on thymus cell migrants. *Nature (Lond.)* 276:79.
- Scollay, R., E. Butcher, and I.L. Weissman. 1980. Thymus cell migration. Quantitative aspects of cellular traffic from the thymus to the periphery in mice. *Eur. J. Immunol.* 10:210.
- Egerton, M., K. Shortman, and R. Scollay. 1990. The kinetics of immature thymocyte development *in-vivo*. *Int. Immunol.* 2:501.
- Egerton, M., R. Scollay, and K. Shortman. 1990. Kinetics of mature T-cell development in the thymus. *Proc. Natl. Acad. Sci. USA.* 87:2579.
- Baron, C., and C. Penit. 1990. Study of the thymocyte cell cycle by bivariate analysis of incorporated bromodeoxyuridine

- and DNA content. *Eur. J. Immunol.* 20:1231.
23. Spangrude, G., and R. Scollay. 1990. Differentiation of hematopoietic stem cells in irradiated mouse thymic lobes. Kinetics and phenotype of progeny. *J. Immunol.* 145:3661.
 24. Terstappen, L.W., S. Huang, and L.J. Picker. 1992. Flow cytometric assessment of human T-cell differentiation in thymus and bone marrow. *Blood.* 79:666.
 25. Swerdlow, S.H., P.A. Angermeier, and A.L. Hartman. 1988. Intrathymic ontogeny of the T cell receptor associated CD3 (T3) antigen. *Lab. Invest.* 58:421.
 26. Hori, T., C. Cupp, N. Wrighton, F. Lee, and H. Spits. 1991. Identification of a novel human thymocyte subset with a phenotype of CD3⁻CD4⁺CD8 α ⁺ β ⁻. Possible progeny of the CD3⁻CD4⁻CD8⁻ subset. *J. Immunol.* 146:4078.
 27. Merckenschlager, M., and A.G. Fisher. 1992. Human postnatal thymocytes generate phenotypically immature CD3dim, CD5dim, CD1a bright progeny in organ culture. *J. Immunol.* 148:1012.
 28. Denning, S.M., D.M. Jones, R.E. Ware, K.J. Weinhold, M.B. Brenner, and B.F. Haynes. 1991. Analysis of clones derived from human CD7⁺CD4⁻CD8⁻CD3⁻ thymocytes. *Int. Immunol.* 10:1015.
 29. Denning, S.M., J. Kurtzenberg, D.S. Leslie, and B.F. Haynes. 1989. Human postnatal CD4⁻CD8⁻CD3⁻ thymic T cell precursors differentiate in vitro into T cell receptor gamma-bearing cells. *J. Immunol.* 142:2988.
 30. Hori, T., and H. Spits. 1991. Clonal analysis of human CD4⁺CD8⁻CD3⁻ thymocytes highly purified from postnatal thymus. *J. Immunol.* 146:2116.
 31. Rouse, R.V., W. van Ewijk, P.P. Jones, and I.L. Weissman. 1979. Expression of MHC antigens by mouse thymic dendritic cells. *J. Immunol.* 122:2508.
 32. van Ewijk, W. 1991. T-cell differentiation is influenced by thymic microenvironments. *Annu. Rev. Immunol.* 9:591.
 33. Haynes, B.F. 1990. Human thymic epithelium and T cell development, current issues and future directions. *Thymus.* 16:143.
 34. de la Hera, A., W. Marston, C. Aranda, M.L. Toribio, and C.A. Martinez-A. 1989. Thymic stroma is required for the development of human T cell lineages in vitro. *Int. Immunol.* 1:471.
 35. Merckenschlager, M., and A.G. Fisher. 1992. Selective manipulation of the human T-cell receptor repertoire expressed by thymocytes in organ culture. *Proc. Natl. Acad. Sci. USA.* 89:4255.
 36. Fisher, A.G., L. Larson, L.K. Goff, D.E. Restall, L. Happerfield, and M. Merckenschlager. 1990. Human thymocyte development in mouse organ cultures. *Int. Immunol.* 2:571.
 37. McCune, J.M., R. Namikawa, H. Kaneshima, L.D. Shultz, M. Lieberman, and I.L. Weissman. 1988. The SCID-hu mouse: murine model for the analysis of human hematolymphoid differentiation and function. *Science (Wash. DC).* 241:1632.
 38. McCune, J.M., H. Kaneshima, M. Lieberman, I.L. Weissman, and R. Namikawa. 1989. The SCID-hu mouse: current status and potential applications. *Curr. Top. Microbiol. Immunol.* 152:183.
 39. Waller, E.K., A.S. Majumdar, M.R. Shick, O.W. Kamel, G.A. Hansteen, and I.L. Weissman. 1992. Human T-cell development in SCID-hu mice: staphylococcal enterotoxins induce specific clonal deletions, proliferation and anergy. *Blood.* 80:3144.
 40. Waller, E.K., O.S. Kamel, M.L. Cleary, A.S. Majumdar, M.R. Shick, M. Lieberman, and I.L. Weissman. 1991. Growth of primary T-cell non-Hodgkin's lymphomata in SCID-hu mice: requirement for a human lymphoid microenvironment. *Blood.* 78:2650.
 41. Spangrude, G.J., S. Heimfeld, and I.L. Weissman. 1988. Purification and characterization of mouse hematopoietic stem cells. *Science (Wash. DC).* 241:58.
 42. Battye, F.L., and K. Shortman. 1991. Flow cytometry and cell-separation procedures. *Curr. Op. Immunol.* 3:238.
 43. Parks, D.R., R.R. Hardy, and L.A. Herzenberg. 1983. Dual immunofluorescence—new frontiers in the analysis and sorting. *Immunol. Today.* 4:145.
 44. Hollander, Z., and M.R. Loken. 1988. Simultaneous analysis of DNA content and surface antigens in human bone marrow. *Cytometry.* 9:485.
 45. Melnicoff, M.J., P.S. Morahan, B.D. Jensen, E.W. Breslin, and P.K. Horan. 1988. In vivo labeling of resident peritoneal macrophages. *J. Leukocyte Biol.* 43:387.
 46. Horan, P.K., S.E. Slezak, and B.D. Jensen. 1993. Cellular proliferation history by fluorescent analysis: *In Flow Cytometry.* A. Jacquemin-Sablon, editor. NATO ASI Series H67. In press.
 47. Civin, C.I., L.C. Strauss, C. Brovall, M.J. Fackles, J.F. Schwartz, and J.H. Shapes. 1984. Antigenic analysis of hematopoiesis. III. A hematopoietic progenitor cell surface antigen defined by a monoclonal antibody raised against KG-1a cells. *J. Immunol.* 133:157.
 48. Namikawa, R., K. N. Weillbaecher, H. Kaneshima, E.J. Yee, and J.M. McCune. 1990. Long-term human hematopoiesis in the SCID-hu mouse. *J. Exp. Med.* 172:1055.
 49. Katsura, Y.T., K. Tatsuo, T. Amagai, T. Tsubata, K. Hirayoshi, Y. Takaoki, T. Sado, and S. Nishirawa. 1986. Limiting dilution analysis of the stem cells for T cell lineage. *J. Immunol.* 137:2434.
 50. Roncarolo, M.G., and B. Vandekerckhove. 1992. SCID-hu mice as a model to study tolerance after fetal stem cell transplantation. *Bone Marrow Transplant.* 9:(Suppl.)1:83.
 51. Arase, H., N. Fukushi, S. Hatakeyama, K. Ogasawara, K. Iwabuchi, C. Iwabuchi, B. Negishi, R.A. Good, and K. Onoe. 1990. Sequential analysis of the thymocyte differentiation in fully allogeneic bone marrow chimera in mice. II. Further characterization of the CD4⁺ or CD8⁺ single positive thymocytes. *Immunobiology.* 180:167.
 52. Vandekerckhove, B.A., R. Namikawa, R. Bacchetta, and M.G. Roncarolo. 1992. Human hematopoietic cells and thymic epithelial cells induce tolerance via different mechanisms in the SCID-hu mouse thymus. *J. Exp. Med.* 175:1033.
 53. Wineman, J.P., G.L. Gilmore, C. Gritzmacher, B.E. Torbett, and C.E. Muller-Sieburg. 1992. CD4 is expressed on murine pluripotent hematopoietic stem cells. *Blood.* 80:1717.
 54. Sen-Majumdar, A., M. Lieberman, S. Alpert, I.L. Weissman, and M. Small. 1992. Differentiation of CD3⁻CD4⁺CD8⁻ thymocytes in short term thymic stromal cell culture. *J. Exp. Med.* 176:543.
 55. Fujiwara, H., M. Ogata, Y. Mizushima, Y. Tatsumi, Y. Takai, and T. Hamaoka. 1990. Proliferation and differentiation of immature thymocytes induced by a thymic stromal cell clone. *Thymus.* 16:159.
 56. Bryant, B.J. 1972. Renewal and fate in the mammalian thymus. Mechanisms and inferences of thymocytokinetics. *Eur. J. Immunol.* 2:38.
 57. Hugo, P., G.A. Waanders, R. Scollay, H.T. Petrie, and R.L. Boyd. 1989. Ontogeny of a novel CD4⁺CD8⁻CD3⁻ thymocyte subpopulation: a comparison with CD4⁻CD8⁺CD3⁻ thymocytes. *Int. Immunol.* 2:209.
 58. Matsumoto, K., Y. Yoshikai, G. Matsuzaki, A. Asano, and K. Nomoto. 1989. A novel CD3⁻ J11d⁺ subset of

- CD4⁺CD8⁻ cells repopulating thymus in radiation bone marrow chimeras. *Eur. J. Immunol.* 19:1203.
59. Matsumoto, K., Y. Hoshikai, Y. Moroi, T. Asano, T. Ando, and K. Nomoto. 1991. Two differential pathways from double-negative to double-positive thymocytes. *J. Immunol.* 72:20.
 60. Hugo, P., G.A. Waanders, R. Scollay, H.T. Petrie, and R.L. Boyd. 1991. Characterization of immature CD4⁺CD8⁻CD3⁻ thymocytes. *Eur. J. Immunol.* 14:2980.
 61. Tanaka, K.E., W.C. Hatch, Y. Kress, R. Soeiro, T. Calvelli, W.K. Rashbaum, A. Rubinstein, and W.D. Lyman. 1992. HIV-1 infection of human fetal thymocytes. *J. Acquired Immune Deficiency Syndromes.* 5:94.
 62. Namikawa, R., H. Kaneshima, M. Lieberman, and I.L. Weissman. 1988. Infection of the SCID-hu mouse by HIV-1. *Science (Wash. DC).* 242:1684.
 - 62a. Bohyhadi, M., L. Rabin, S. Salimi, D. Brown, J. Kosek, M. McCune, and H. Kaneshima. Prophylactic and postexposure effects of DDI on HIV-associated pathology in HIV-1 infected human fetal Thy/Liv implants in SCID-hu mice. 22nd Annual Keystone Symposium. *J. Cell. Biochem. Suppl.* 17E:12.
 63. Richie, E.R., B.B. McEntire, L. Coghlan, and M. Poenie. 1991. Murine T-lymphomas corresponding to the immature CD4⁻8⁺ thymocyte subset. *Dev. Immunol.* 1:255.
 64. Waller, E.K., M. Ziemnanska, C.D. Bangs, M. Cleary, I.L. Weissman, and O. Kamel. 1993. Characterization of post-transplant lymphomas that express T-cell associated markers: immunophenotypes, molecular genetics, cytogenetics and heterotransplantation in SCID mice. *Blood.* In press.
 65. Shortman, K., D. Vremec, and M. Egerton. 1991. The kinetics of T cell antigen receptor expression by subgroups of CD4⁺8⁺ thymocytes: delineation of CD4⁺8⁺32⁺ thymocytes as post-selection intermediates leading to mature T cells. *J. Exp. Med.* 173:322.
 66. London, N.J.M., S.M. Thirdborough, S.M. Swift, P.R.F. Bell, and R.F.L. James. 1991. The diabetic "human reconstituted" severe combined immunodeficient (SCID-hu) mouse: model for isogeneic, allogeneic, and xenogeneic human islet transplantation. *Transplant. Proc.* 23:749.